A Compact Coaxial Waveguide Combiner Design For Ultra-Broadband Power Amplifiers

Pengcheng Jia, Robert A. York
E.C.E. Dept., University of California, Santa Barbara, CA 93106, USA

***Abstract* — We report an enhanced broadband passive combiner structure using a dense slot-line antenna array in an oversized coaxial waveguide. A significant reduction in size has been achieved while maintaining a 6-18GHz bandwidth and capacity for 32 MMIC amplifiers. A broadband slotline to microstrip line transition is also developed and monolithically integrated with the slot-line antennas, to eliminate a troublesome bond-wire transition in earlier design and provide better compatibility with commercial MMICs. The Spectral Domain Method (SDM) is applied to compute the field in the structure, and small reflection theory is extended to synthesize the waveguide taper and optimized slotline taper array.**

I. INTRODUCTION

Waveguide-based spatial power combiners using finline arrays are good candidates for high power broadband combining [1-2]. In this approach, the combiner is implemented in a "tray" architecture, which permits the use of broadband antennas and improved functionality through circuit integration along the direction of propagation. Each tray consists of a number of tapered slotline or finline transitions, which coupled energy to and from a waveguide aperture to a set of MMIC amplifiers. The use of the waveguide mode to distribute and collect energy to and from the set of amplifiers thus avoids loss mechanisms that limit the efficiency in corporate combiner structures.

A rectangular waveguide power combiner has achieved 120-Watt output power over X-Band [1]. The bandwidth of rectangular waveguide combiners is limited by the cutoff frequency of the waveguide. To fully exploit the inherently wide bandwidth of a slotline antenna array, a coaxial waveguide combiner is developed. In this case the slotline array is loaded radially inside the opening of an oversized coaxial waveguide. Preliminary results demonstrated over 12 GHz bandwidth in a prototype passive structure [3]; this was subsequently integrated with 32 broadband traveling-wave amplifier MMICs [4], demonstrating high combining efficiency of >75%.

As shown in Fig. 1, the center section of the coaxial waveguide combiner is enlarged to accommodate the slotline array and MMICs. Coaxial waveguide tapers are applied at both ends of the center section, providing transition from the enlarged center section to standard N connectors. Our previous design was undesirably large in both the diameter of the center section and the length of waveguide taper. A new compact system, which provides the same performance as the larger one, was developed and reported here.

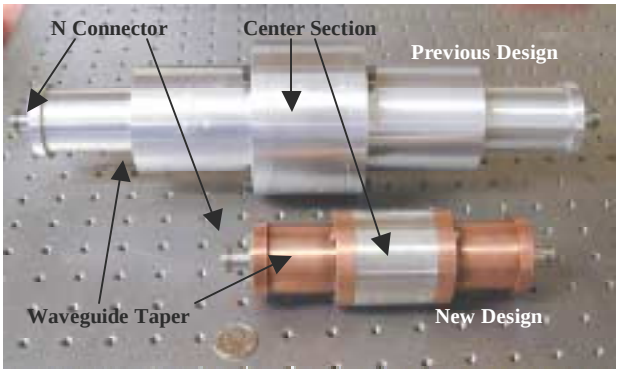

Fig. 1. Comparison between previous design and the new compact design.

For low power demonstrations, the MMICs were die-attached directly to the AlN substrate supporting the slot-line antennas. For high power modules, the MMICs must be attached to the metal carrier for better thermal management, as in [1]. A slotline to microstrip line transition is therefore necessary for connection between slotline antenna and the commercial MMICs. In [1-2], a separate microstrip line was bonded to the end of slotline with hybrid wire bonding. The wire bonding adds parasitic inductance to the transition, and increase the difficulty in fabricating the system. A monolithic broadband transition is developed in this paper to eliminate the parasitic effect. The new transition can retain the same bandwidth. Furthermore, it can be easily extended to higher frequencies.

II. COAXIAL WAVEGUIDE DESIGN

The primary goal of the work is to re-engineer the combiner to minimize the physical size, while maintaining a large amplifier capacity, wide bandwidth (6-18GHz is

the goal), and good thermal capacity. We succeed in reducing the diameter of the center section from 4 inch to 2.2 inch, and the length of each waveguide taper is reduced from 6.2 inch to 2.2 inch.

A smaller waveguide impedance leads to smaller aperture, which is helpful in suppressing higher order modes. When slotlines are loaded in the waveguide, the input impedance of each slotline is the number of channels times the waveguide impedance. Lower waveguide impedance can keep the slotline taper shorter, which means lower conductive loss. The impedance of the center section was chosen to be 30 Ohm, with an outer diameter of the coaxial waveguide opening of 0.8 inch.

The reflection from the N-connector to flared waveguide line is minimized by the optimized coaxial waveguide transition. The gradual waveguide taper is synthesized from small reflection theory of TEM lines, and has an input reflection coefficient

$$\Gamma_{in}(f) = \frac{1}{2}\int_0^{\theta_t} e^{-j\theta}\frac{d}{d\theta}\ln\left(\frac{Z(\theta)}{Z_0}\right)d\theta . \qquad (1)$$

where z is the position along the taper, L is the taper length, β is the propagation constant, Z_0 represents the reference impedance at the input end of the taper, and $\theta = 2\beta dz$ is the round-trip phase delay to a point z along the taper, $\theta_t = 2\beta L$.

In order to maintain an input reflection coefficient $\Gamma < \Gamma_m$ over the desired bandwidth, it has been shown in [5,6] that $Z(\theta)$ must take the form

$$\ln\frac{Z(\theta)}{Z_0} = \frac{1}{2}\ln\frac{Z_L}{Z_0} + \Gamma_m A^2 F\left(\frac{2\theta}{2\theta_t} - 1, A\right). \qquad (2)$$

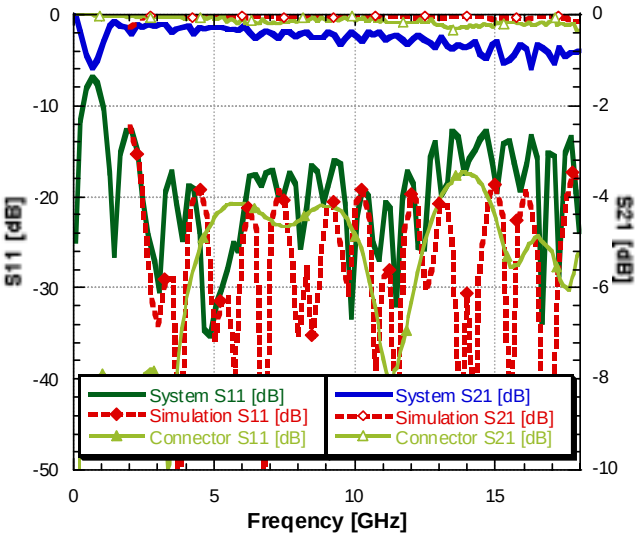

Fig. 2. S parameter of unloaded coaxial waveguide.

The simulation and measurement results of the unloaded compact coaxial waveguide are shown in Fig. 2. There is no solder or epoxy used in assembling the system. The center conductor of the combiner is designed to mate directly to the center conductor of a type-N connector for easy assembly, but this also introduced additional loss and reflection. And 2 N-to-SMA connectors are used for measurement, which is not considered in simulation. The loss and reflection of the N-to-SMA connector is also shown in Fig. 2. It contributes to the discrepancy between simulation and measurement.

III. SYNTHESIS OF WAVEGUIDE SLOTLINE ARRAY

16 slotline trays are radially loaded inside the center waveguide opening. The symmetry and the thinness of circuit substrate allow us to focus analytical attention on a $1/16^{th}$ unit cell. The $1/16^{th}$ cell is then further approximated by a parallel-plate waveguide [3]. The Spectral Domain Method is applied to compute the field. The propagation constant and impedance are computed by an iteration process. Then the small reflection theory is used again to optimize the slotline taper, with β as a function of the slotline gap and frequency. The detailed modeling work is elaborated in [4]. Fig. 3 shows the layout of the slotline taper.

Each circuit tray carries 2 slotline tapers. To improve the linearity of the combiner, power should be distributed evenly to each taper. But the field inside the waveguide is not radially uniform. So each of the 2 tapers on each tray is designed with a different opening to equalize the power. When we put the slotline tray inside the waveguide, they will have same outer radius to inner radius ratio.

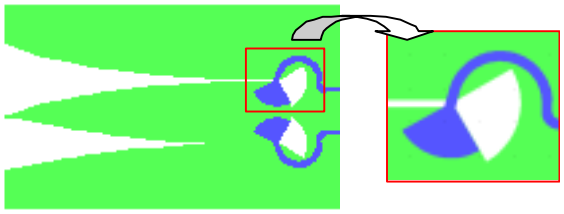

Fig. 3. Layout of the slotline taper and the slotline to microstrip line transition

IV. SLOTLINE TO MICROSTRIP LINE TRANSITION

In the previous design, a separate microstrip transition is adopted to provide connection from the end of slotline to MMICs. The microstrip line and slotline are not in the same plane, bonding wire is needed for interconnection. It is hard to keep the wire very short in fabrication. To avoid

parasitic inductance, a monolithic slotline to microstrip transition is employed in the new design [7].

As shown in Fig. 3, the slotline is processed on the back of the AlN substrate, with a 90-degree slotline short stub at the end. A 90-degree microstrip open stub is aligned to the slotline stub on the top of the substrate. The center of the 2 stubs are on the same line perpendicular to the surface, and their edges are parallel to each other. When put onto a metal carrier, the slotline become the ground of microstrip line, which is also the ground of MMICs. Due to the space limitation inside the compact structure, the stubs have to be bended 30-degree inwards, and the microstrip line detours around the slotline stub in a small loop.

The transition in Fig. 3 is modeled in Fig. 4.

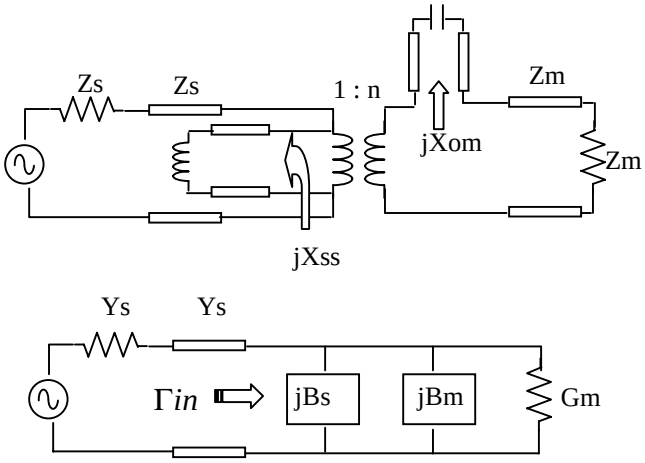

Fig. 4. Circuit model of slotline to microstrip line transition.

The short slotline stub and open microstrip stub can be treated as a series of straight sections of various width that are cascaded together [8]. To improve the accuracy of structure enclosed in waveguide, we use 3D simulator Agilent HFSS to compute the reactance of the slotline stub jXss and microstrip stub jXom. Then we apply the values into the circuit model and optimize other parameters in the transition. In the circuit model, Zm and Zs is the characteristic impedance of microstrip line and slotline, n is the transformer ratio,

$$n = -\frac{1}{Vo}\int_{-\frac{b}{2}}^{\frac{b}{2}} Ey(h)dy,$$

$$Ey(h) = -\frac{Vo}{b}(\cos\frac{2\pi u}{\lambda o}h - \cot q_o \sin\frac{2\pi u}{\lambda o}h), \tag{3}$$

$$Gm = \frac{n^2 Zm}{Zm^2 + Xom^2}, \qquad Ys = \frac{1}{Zs},$$

$$Bm = -\frac{n^2 Xom}{Zm^2 + Xom^2}, \qquad Bs = -\frac{1}{Xss}.$$

Vo is the voltage across the slot and Ey(h) is the electric field of the slotline on the other surface of the substrate. The details of the calculation of n are in [9]. The

$$\Gamma in = \frac{Ys - Gm - j(Bs + Bm)}{Ys + Gm + j(Bs + Bm)}. \tag{4}$$

reflection coefficient can be expressed as:

Our goal is to achieve bandwidth from 6 to 18GHz. Simulation shows that the lower band is more sensitive to the parameters. So we choose 10GHz as the center frequency, optimize the transition to satisfy Ys=Gm, and Bs=-Bm.

The microstrip line is fixed to be 50 Ohm, corresponding to 278 um strip width on a 254 um thick AlN substrate. The characteristic impedance of the slotline times n^2 should be close to 50 Ohm. We choose the width of the slotline to be 40 um to match Ys with Gm. Due to the limitation of the space inside the waveguide structure, the radius of the slotline stub is selected to be 2000 um. To realize Bs=-Bm and minimize the reflection coefficient, the microstrip open stub should have a radius of 1500 um. Further optimization with Agilent HFSS shows that microstrip stub with 1600 um radius have a wider bandwidth. Simulation result indicates that the slotline to microstrip transition can achieve a bandwidth of 12 GHz, from 6 to 18 GHz. If scaled down properly, the transition can also work at higher bands. The parasitic effect is much smaller than the bonding wire connection used in earlier work.

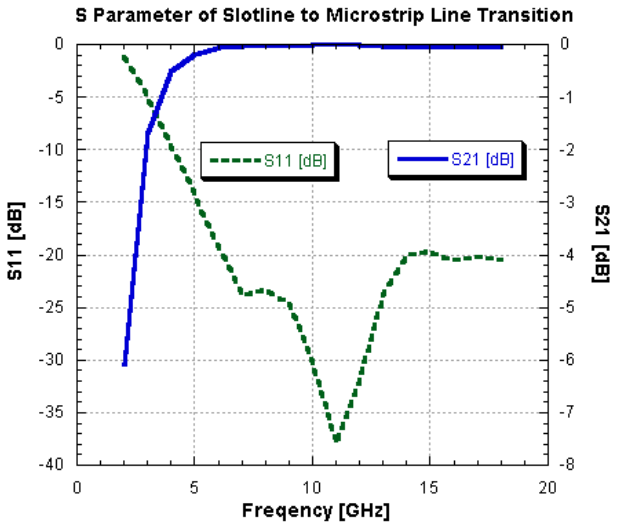

Fig. 5. S parameter of slotline to microstrip line transition from Agilent HFSS simulation

V. Compact Passive structure of Coaxial waveguide combiner

Fig. 6 shows the open view of the combiner, which integrates coaxial waveguide with circuit trays. The circuit tray for loss and impedance match measurement is also shown in Fig. 6. It has 2 patterns as shown in Fig. 3, placed back to back. Slots are machined on the walls of the center flared coaxial waveguide, and circuit trays are slided into it. Coaxial waveguide tapers with N-connectors are connected to both sides. The performance of the overall system is shown in Fig. 7.

Fig. 6. Open view of the passive coaxial waveguide combiner.

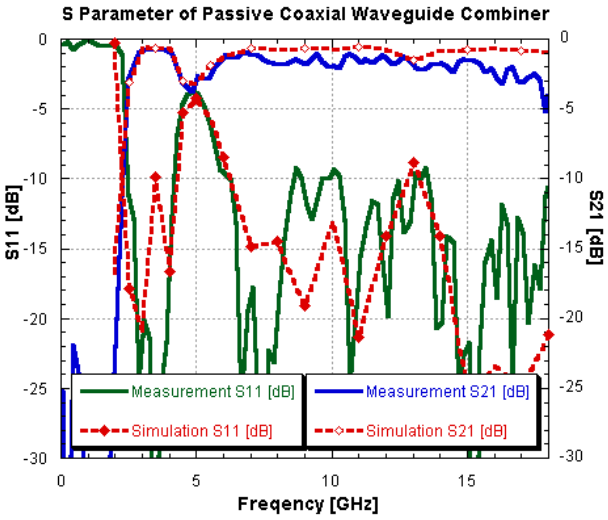

Fig. 7. Comparison between simulation and measurement for passive coaxial waveguide combiner.

VI. Conclusion

A compact coaxial waveguide combiner structure is presented in this paper. The total size of the new system is reduced dramatically compared to previous ones. And with the monolithic integration of the microstrip to slotline transition, fabrication of the system becomes easier with better performance. Furthermore, the new transition makes it possible to extend the structure to higher frequencies.

Acknowledgement

The authors wish to acknowledge the assistance and support of Paolo F. Maccarini. This work is funded through the ONR MURI IMPACT program (grant N00014-96-1-1215), and by an ARO MURI program (grant DAAG55-98-1-0001).

References

[1] N. –S. Cheng, P. Jia, D. B. Rensch and R. A. York, “A 120-Watt X-Band Spatially Combined Solid-State Amplifier”, *IEEE Trans. Microwave Theory and Tech.*, Vol. MTT-47, No.12, pp. 2557-61, Dec 1999.

[2] P. Jia, L.-Y. Chen, N.-S. Cheng, and R.A. York, “Design of Waveguide Finline Arrays for Spatial Power Combining”, to be published on *IEEE Trans. Microwave Theory and Tech.*.

[3] P. Jia, Y. Liu, R.A. York, “Analysis of A Passive Spatial Combiner Using Tapered Slotline Array in Oversized Coaxial Waveguide” *2000 IEEE MTT-S International Microwave Symposium Digest*, Boston, MA, USA, pp.1933-6, Vol.3, June 2000.

[4] P. Jia, L.-Y. Chen and R.A. York, “Ultra-Broadband Coaxial Waveguide Power Combiner”, submitted to *IEEE Trans. Microwave Theory and Tech.*.

[5] D. M. Pozar, *Microwave Engineering*, 2nd Ed., New York, NY: John Wiley & Sons, 1998.

[6] R.W. Klopfenstein, “A Transmission-Line Taper of Improved Design,” *Proc. IRE*, vol. 442, pp. 31-35, January 1956.

[7] M.M. Zinieris, R. Sloan, and L.E. Davis, “ A Broadband Microstrip-To-Slot-Line Transition”, *Microwave and Optical Technology Letters*, vol 18, No. 5, pp 339-342 August 1998.

[8] B. Schuppert, “Microstrip/Slotline Transitions: Modeling and Experimental Investigation”, IEEE *Trans. Microwave Theory and Tech.*, Vol. 36, 1988, pp. 1272-1282.

[9] K.C. Gupta, R. Garg, and I.J. Bahl, *Microstrip Lines and Slotlines*, Artech House, Norwood, MA, 1979.